Simultaneous Distributed Localization and Formation Tracking Control via Matrix-weighted Position Constraints

Xu Fang [a,b,c], Lihua Xie [b], Dimos V. Dimarogonas [c]

[a] *Key Laboratory of Intelligent Control and Optimization for Industrial Equipment of Ministry of Education, Dalian University of Technology, Dalian 116024, China*

[b] *School of Electrical and Electronic Engineering, Nanyang Technological University, 639798, Singapore*

[c] *School of Electrical Engineering and Computer Science, KTH Royal Institute of Technology, Stockholm SE-10044, Sweden*

Abstract

This paper studies the problem of 3-D relative-measurement-based leader-follower simultaneous distributed localization and formation tracking control. The position information is only available to the leaders, and the followers have inter-agent relative measurements and communication with their neighbors. The key contribution is the development of a weight-matrix-based position constraint, which can make use of relative measurements such as bearing, ratio-of-distance, angle, distance, relative position and their mixture to describe the position relationship among each follower and its neighbors in 3-D space. A bearing-based distributed protocol is proposed for each follower to estimate its position and track its target position, which can drive the followers from their unlocalizable positions to localizable positions. The proposed algorithm is then extended to the case that both bearing and ratio-of-distance measurements are available, where the followers are localizable at all times if the followers and their neighbors are not collocated. In addition, the proposed method is also applicable to homogeneous or heterogeneous angle, distance, and relative position measurements as the ratio-of-distances or bearings can be obtained indirectly by these relative measurements. A remarkable advantage is that the proposed method can be implemented without persistently exciting motions. Some illustrative simulations are presented to verify the theoretical results.

Key words: Formation tracking control, distributed localization, bearing, ratio-of-distance, multi-agent system, 3-D space.

1 Introduction

Network localization and formation tracking control for multi-agent systems enjoys wide application in civilian and military applications such as the well-studied target entrapping (Yang et al., 2021, 2020). In leader-follower multi-agent systems, network localization aims to localize the followers based on the leaders' positions and relative measurements. The widely used inter-agent relative measurements in distributed network localization are: distances (Eren et al., 2004; Aspnes et al., 2006; Khan et al., 2009), angles (Jing et al., 2022), bearings (Shames et al., 2012; Le-Phan et al., 2023; Zhao and Zelazo, 2016), and their mixture (Barooah and Hespanha, 2007). Different from network localization, formation tracking control aims to track target moving formations based on inter-agent relative measurements and communication.

In this article, we focus on utilizing homogeneous or heterogeneous relative measurements (such as bearing or ratio-of-distance measurement) to achieve simultaneous distributed localization and formation tracking control. Most of the existing bearing-based research only studies formation tracking control (Trinh and Ahn, 2021). Note that the global (absolute) positions of the agents are also important in certain application tasks such as map construction and source seeking (Chen et al., 2022). Hence, there is a need of a simultaneous network localization and formation tracking control scheme.

However, the bearing-based simultaneous network localization and formation tracking control problem cannot be solved trivially by combining the existing bearing-

⋆ This work was partially supported by the Wallenberg AI, Autonomous Systems and Software Program (WASP) funded by the Knut and Alice Wallenberg Foundation and Ministry of Education, Singapore, under AcRF TIER 1 Grant RG64/23. (Corresponding author: Lihua Xie.)

Email addresses: fa0001xu@e.ntu.edu.sg (Xu Fang), elhxie@ntu.edu.sg (Lihua Xie), dimos@kth.se (Dimos V. Dimarogonas).

based network localization (Shames et al., 2012; Le-Phan et al., 2023; Zhao and Zelazo, 2016) and formation tracking control approaches (Trinh et al., 2018; Zhao et al., 2019; Van Tran et al., 2018b). The reason is that the existing bearing-based network localization methods require the network to be non-degenerate, e.g., each follower and its neighbors are non-collinear or the network is infinitesimally bearing rigid at all times (Le-Phan et al., 2024; Van Tran et al., 2018a; Zhao and Zelazo, 2019), which is challenging to ensure. Thus, the first technical challenge is how to realize bearing-based distributed localization in multi-agent systems with dynamic (moving) agents.

To tackle this problem, the existing works (Yang et al., 2021; Ye et al., 2017; Tang and Loría, 2022; Su et al., 2023; Zhu et al., 2023) usually require the agents to keep persistently exciting motions. The persistently exciting motions in (Yang et al., 2021; Ye et al., 2017; Tang and Loría, 2022; Su et al., 2023; Zhu et al., 2023) are mainly used for the agents to achieve self-localization, which restrict the design of desired target formation. Also, they may increase the agents' energy consumption. For example, the agents need not only to perform translational motions for target tracking, but also require additional circular motions for localization (Ye et al., 2017). Thus, the second technical challenge is how to realize bearing-based distributed localization and control in a motion-excitation-free manner. Although our complex-Laplacian-based approach does not require persistently exciting motions (Fang et al., 2023), it can only be applied in 2-D plane and needs additional distance measurements. In addition, the existing orthogonal-matrix-based position constraint (Zhao and Zelazo, 2016) is only applicable to bearing measurements. The third technical challenge is to propose a general position constraint, which can accommodate different relative measurements for distributed localization and formation control.

To deal with the above challenges, in this article, we propose a 3-D simultaneous network localization and formation tracking control algorithm. The main contributions and novelty are summarized as follows:

(i) Different from the bearing-based orthogonal projection matrix (Zhao and Zelazo, 2016), a relative-measurement-based weight matrix is proposed to describe the position relationship among each follower and its neighbors in 3-D space. The proposed weight matrix is not only applicable to bearing measurements, but also applicable to ratio-of-distance, relative position, distance, angle, and their mixture.

(ii) Based on the weight-matrix-based position constraint, a 3-D bearing-based simultaneous distributed localization and formation tracking control protocol is proposed for the followers to achieve self-localization and track their target positions. The proposed algorithm is then extended to the case where both bearing and ratio-of-distance measurements are available. Different from motion-excitation-based methods (Yang et al., 2021; Ye et al., 2017; Tang and Loría, 2022; Su et al., 2023; Zhu et al., 2023), the proposed approach can be implemented in a motion-excitation-free manner, i.e., the agents are not required to keep persistently exciting motions.

(iii) Different from the existing bearing-based localization approaches which require the agents to be localizable at all times (Shames et al., 2012; Le-Phan et al., 2023; Zhao and Zelazo, 2016), the proposed bearing-based protocol can drive the followers out of unlocalizable positions and get them to their target positions. In the bearing-ratio-of-distance-based distributed protocol, each follower is localizable at all times if each follower and its neighbors are not collocated, i.e., each follower is localizable even if it is collinear with its neighbors.

(iv) The sum of the squares of the estimation and tracking errors of the followers will not increase when there are occlusions in the environment or the followers are in unlocalizable regions. In addition, the bearing-based or bearing-ratio-of-distance-based distributed protocol can be extended to homogeneous or heterogeneous angle, distance, and relative position measurements.

The organization of this article is as follows. Section 2 introduces the notations and formulates the problem. The concept of weight-matrix-based position constraint is introduced in Section 3. Two distributed protocols are presented in Section 4 to realize self-localization and track the desired position simultaneously. Some simulations are given in Section 5 to verify the theoretical results. Conclusions are drawn in Section 6.

2 Notations and Problem Statement

2.1 Notations

The set of real numbers and positive real numbers are denoted by $\mathbb{R}$ and $\mathbb{R}^+$, respectively. The identity matrix is denoted by $I_d \in \mathbb{R}^{d\times d}$. Let $|\cdot|$ be the absolute value of a given real number. Denote by $\mathbf{1}_d, \mathbf{0}_d \in \mathbb{R}^d$ the column vectors with all entries equal to one and zero, respectively. Let $\|\cdot\|_1$ and $\|\cdot\|_2$ be the L_1-norm and L_2-norm of a given matrix or vector, respectively. Let $\det(\cdot)$ be the determinant of a given square matrix. A communication graph $\mathcal{G}$ is a pair of $\{\mathcal{V}, \mathcal{E}\}$, where $\mathcal{V}$ is a nonempty finite set of agents and $\mathcal{E} \subseteq \mathcal{V} \times \mathcal{V}$ is a set of edges. Agent j is called a neighbor of agent i if $(i, j) \in \mathcal{E}$. Denote by $\mathcal{A}^T$ the transpose of a matrix $\mathcal{A} \in \mathbb{R}^{d\times d}$ or a vector $\mathcal{A} \in \mathbb{R}^d$. Denote by $\mathcal{A} \in [\mathbb{R}]^{k_1\times k_2}_{d\times d}$ a block matrix with k_1 row block partitions and k_2 column block partitions, where each block is a submatrix of dimension $d \times d$. That is, the block matrix $\mathcal{A} \in [\mathbb{R}]^{k_1\times k_2}_{d\times d}$ is a matrix of dimension

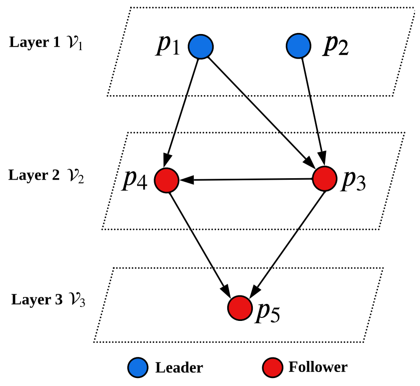

Fig. 1. A directed graph.

$k_1d \times k_2d$. For example,

$$\mathcal{A} = \begin{bmatrix} A_{11} & A_{12} \\ A_{21} & A_{22} \end{bmatrix} \in [\mathbb{R}]^{2\times 2}_{3\times 3} = \mathbb{R}^{6\times 6}, \tag{1}$$

where the block matrix $\mathcal{A}$ in (1) has 2 row block partitions and 2 column block partitions, and $A_{11}, A_{12}, A_{21}, A_{22} \in \mathbb{R}^{3\times 3}$ are the matrices of dimension 3×3.

Consider a group of n mobile agents in $\mathbb{R}^3$, where $p_i = [x_i, y_i, z_i]^T \in \mathbb{R}^3$ represents the position of agent i in 3-D space and $p = [p_1^T, \cdots, p_n^T]^T \in \mathbb{R}^{3n}$ is the configuration of all agents. A formation is denoted by $(\mathcal{G}, p)$. Suppose there are m leaders and $n-m$ followers. The set of leader group and follower group are denoted by $\mathcal{V}_l = \{1, \cdots, m\}$ and $\mathcal{V}_f = \{m+1, \cdots, n\}$, respectively. The positions of leader group and follower group are denoted by $p_l = [p_1^T, \cdots, p_m^T]^T$ and $p_f = [p_{m+1}^T, \cdots, p_n^T]^T$, respectively. The 3-D inter-agent bearing g_{ij} in the global coordinate frame and ratio-of-distance r_{ijk} for the non-collocated agents i, j, k are represented by

$$g_{ij} = \frac{p_{ij}}{\|p_{ij}\|_2}, \quad r_{ijk} = \frac{\|p_{ij}\|_2}{\|p_{ik}\|_2}, \tag{2}$$

where $p_{ij} = p_j - p_i$ is the relative position between agent i and agent j. Let $\hat{p}_i$ be the position estimate of agent i. The angle θ_i for the non-collocated agents i, j, k is represented by $\theta_i = \arccos(g_{ij}^T g_{ik})$.

2.2 Graph Design

The directed graph $\mathcal{G}$ in this article is designed based on the following rules:

(i) The agent set $\mathcal{V}$ of $\mathcal{G}$ consists of $\kappa > 1$ subsets $\mathcal{V}_1, \mathcal{V}_2, \cdots, \mathcal{V}_\kappa$, where $\mathcal{V}_i \cap \mathcal{V}_j = \emptyset$ if $i \neq j$. Agent i is said to be in layer s if $i \in \mathcal{V}_s (1 \leq s \leq \kappa)$. Subset $\mathcal{V}_1$ includes all leaders, i.e., $\mathcal{V}_1 = \mathcal{V}_l$. The union of the subsets $\mathcal{V}_2, \cdots, \mathcal{V}_\kappa$ includes all followers, i.e., $\bigcup_{s=2}^{\kappa} \mathcal{V}_s = \mathcal{V}_f$;

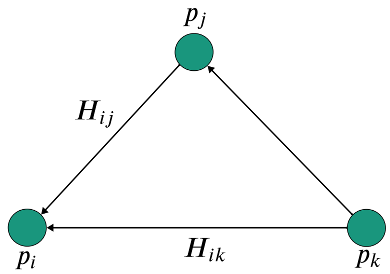

Fig. 2. Example of constructing a weight-matrix-based position constraint.

(ii) There are at least two leaders, and the leaders have no neighbor. Each follower i has at least two neighbors, and the neighbor set N_i of follower i is designed as

$$\mathcal{N}_i = \{j \in \bigcup_{g=1}^{s} \mathcal{V}_g : j < i,\ (i,j) \in \mathcal{E},\ i \in \mathcal{V}_s,\ s > 1\}. \tag{3}$$

An example of the directed graph $\mathcal{G}$ is given in Fig. 1.

2.3 Problem Statement

The dynamics of each agent is

$$\dot{p}_i = u_i,\ i = 1, \cdots, n, \tag{4}$$

where $p_i \in \mathbb{R}^3$ is the position and $u_i \in \mathbb{R}^3$ is the control input. In this article, we aim to localize and control the followers p_f based on the positions of the leaders p_l and inter-agent relative measurements, i.e.,

$$\begin{cases} \lim\limits_{t\to\infty} (\hat{p}_f(t) - p_f(t)) = \mathbf{0}, \\ \lim\limits_{t\to\infty} (p_f(t) - p_f^*(t)) = \mathbf{0}, \end{cases} \tag{5}$$

where $\hat{p}_f$ and p_f^* are, respectively, the position estimate and target position of the follower group. The target trajectory $p_f^*(t)$ is assumed to be first-order differentiable.

3 Bearing-induced Position Relationship

3.1 Weight-matrix-based Position Constraint

If agents i, j, k are not collocated, i.e., $p_i \neq p_j \neq p_k$, a weight-matrix-based position constraint for agents i, j, k is given by

$$H_{ij}(p_j - p_i) + H_{ik}(p_k - p_i) = \mathbf{0},\ i \in \mathcal{V}_f, \tag{6}$$

where $H_{ij}, H_{ik} \in \mathbb{R}^{3\times 3}$ are appropriate weight matrices. The weight matrices H_{ij}, H_{ik} in (6) can be calculated based on the positions p_i, p_j, p_k as shown in Algorithm 2. A simple example of (6) is given in Fig. 2, where the positions of agents i, j, k are $p_i = [0, 0, 0]^T$, $p_j = [2, 1, 1]^T$ and $p_k = [1, 2, 2]^T$. Then, the weight matrices H_{ij}, H_{ik} in (6) are calculated as

$$H_{ij} = \begin{bmatrix} 0.5 & 1.5 & 0 \\ -1.5 & 2.5 & 0 \\ 0 & 0 & 2 \end{bmatrix}, \ H_{ik} = \begin{bmatrix} 0.5 & -1.5 & 0 \\ 1.5 & -0.5 & 0 \\ 0 & 0 & -1 \end{bmatrix}. \quad (7)$$

Equation (6) can be rewritten as

$$H_{ii}p_i = H_{ij}p_j + H_{ik}p_k, \quad (8)$$

where $H_{ii} = H_{ij} + H_{ik}$. If H_{ii} is nonsingular, we have $p_i = H_{ii}^{-1}(H_{ij}p_j + H_{ik}p_k)$. Hence, the weight matrices H_{ij}, H_{ik} describe the position relationship among agents i, j, k. The immediate question is when the matrix H_{ii} is nonsingular.

Remark 1 *As shown in Algorithm 2, the weight matrices H_{ij}, H_{ik} in (6) are calculated based on the plain positions of agents i, j, k, which are different from the bearing-based orthogonal projection matrix in (Zhao and Zelazo, 2016; Trinh et al., 2018).*

Lemma 3.1 *If agents i, j, k are not collocated and the weight matrices H_{ij}, H_{ik} in (6) are calculated based on Algorithm 2, the weight matrix $H_{ii} = H_{ij} + H_{ik}$ is nonsingular, i.e., p_i can be uniquely determined by the positions p_j, p_k in (8).*

The proof of Lemma 3.1 is given in Appendix-B.

Remark 2 *In Fig. 2, the agents i, j, k are not collocated, and we can know from (7) that $H_{ii} = H_{ij} + H_{ik} = I_3$ is nonsingular. Hence, p_i can be uniquely determined by p_j, p_k, i.e., $p_i = H_{ij}p_j + H_{ik}p_k$.*

Definition 1 *The configurations $\check{p} = [p_i^T, p_j^T, p_k^T]^T$ and $\check{q} = [q_i^T, q_j^T, q_k^T]^T$ are translation-scaling similar if they satisfy*

$$\check{q} = \kappa \check{p} + \mathbf{1}_3 \otimes b, \quad (9)$$

where $\kappa \in \mathbb{R}^+$ is a non-zero scaling parameter, $b \in \mathbb{R}^3$ is a translation parameter, and $\otimes$ is the Kronecker product.

Lemma 3.2 *The configurations $\check{q} = [q_i^T, q_j^T, q_k^T]^T$ and $\check{p} = [p_i^T, p_j^T, p_k^T]^T$ have the same weight matrices if they are translation-scaling similar.*

Proof. *From (9), it has*

$$q_i = \kappa p_i + b, \ q_j = \kappa p_j + b, \ q_k = \kappa p_k + b. \quad (10)$$

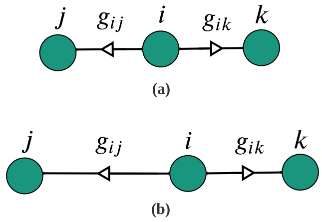

Fig. 3. Agents i, j, k are not collocated but collinear.

Combining (8) and (10), it has

$$\begin{aligned} & H_{ii}q_i - H_{ij}q_j - H_{ik}q_k \\ & = H_{ii}(\kappa p_i + b) - H_{ij}(\kappa p_j + b) - H_{ik}(\kappa p_k + b) \\ & = \kappa(H_{ii}p_i - H_{ij}p_j - H_{ik}p_k) + (H_{ii} - H_{ij} - H_{ik})b \quad (11) \\ & = \kappa(H_{ii}p_i - H_{ij}p_j - H_{ik}p_k) \\ & = \mathbf{0}. \end{aligned}$$

Since $\kappa \neq 0$, from (11), it has

$$H_{ii}p_i - H_{ij}p_j - H_{ik}p_k = \mathbf{0} \Longleftrightarrow H_{ii}q_i - H_{ij}q_j - H_{ik}q_k = \mathbf{0}. \quad (12)$$

It is clear from (12) that the configurations $\check{q} = [q_i^T, q_j^T, q_k^T]^T$ and $\check{p} = [p_i^T, p_j^T, p_k^T]^T$ can have the same weight matrices. □

Definition 2 *A formation $(\mathcal{G}, p)$ is said to be localizable if the followers' positions p_f can be uniquely determined by the leaders' positions p_l through the weight-matrix-based position constraints (6).*

From Lemma 3.2, we can deduce that the proposed weight-matrix-based position constraint between each follower and its neighbors can be obtained if the translation-scaling similar configuration can be calculated based on their relative measurements as shown in subsequent sections.

3.2 Construction of Weight-matrix-based Position Constraint Using Bearing Measurements

There are two cases for the non-collocated agents i, j, k:

(i) If agents i, j, k are not collocated but collinear, the bearings among the agents i, j, k are not only invariant to translation and scaling of p_i, p_j, p_k, but also invariant to some other motions of p_i, p_j, p_k. For example, the agents i, j, k in Fig. 3(a) and Fig.3(b) have the same bearings, but the agents i, j, k in Fig. 3(a) cannot be obtained by the translation and scaling of agents i, j, k in Fig. 3(b). Thus, the geometric shape of agents i, j, k cannot be uniquely determined by the bearings if they are collinear, i.e., agent i cannot be localized by agents j, k. Then, the weight matrices H_{ij}, H_{ik} in (6) are set to $H_{ij} = \mathbf{0}, H_{ik} = \mathbf{0}$, which mean that the position relationship among agents i, j, k is not available.

(ii) If agents i, j, k are non-collinear, the bearings among the agents i, j, k are only invariant to translation and scaling of p_i, p_j, p_k. Thus, the translation-scaling similar configuration of agents i, j, k can be obtained based on the bearings as shown in Algorithm 3. Then, the weight matrices H_{ij}, H_{ik} in (6) can be calculated based on the translation-scaling similar configuration through Algorithm 2. From Lemma 3.1, agent i can be localized by agents j, k.

The weight-matrix-based position constraint of each follower $i \in \mathcal{V}_f$ from (8) can be aggregated into a block matrix form, i.e.,

$$\mathcal{B}_f p = \mathbf{0}, \tag{13}$$

where $p = [p_1^T, \cdots, p_n^T]^T$ and $\mathcal{B}_f \in [\mathbb{R}]_{3\times 3}^{(n-m)\times n}$ in (13) is a block matrix with $n-m$ row block partitions and n column block partitions. Let $[\mathcal{B}_f]_{ij}$ be a block in the ith row block partition $i \in \mathcal{V}_f$ and jth column block partition, i.e.,

$$[\mathcal{B}_f]_{ij} = \begin{cases} H_{ii}, & j = i, \\ 0, & j \notin \mathcal{N}_i,\ j \neq i, \\ -H_{ij}, & j \in \mathcal{N}_i,\ j \neq i, \end{cases} \tag{14}$$

where $H_{ii} = \sum_{k \in \mathcal{N}_i} H_{ik}$. Based on p_l and p_f, the block matrix $\mathcal{B}_f = [\mathcal{B}_{fl}\ \mathcal{B}_{ff}]$ in (13) can be decoupled into

$$\mathcal{B}_{fl} p_l + \mathcal{B}_{ff} p_f = \mathbf{0}, \tag{15}$$

where $\mathcal{B}_{fl} \in [\mathbb{R}]_{3\times 3}^{(n-m)\times m}$ and $\mathcal{B}_{ff} \in [\mathbb{R}]_{3\times 3}^{(n-m)\times (n-m)}$. If the block matrix $\mathcal{B}_{ff}$ in (15) is nonsingular, it has $p_f = -\mathcal{B}_{ff}^{-1} \mathcal{B}_{fl} p_l$. The construction of weight-matrix-based position constraint using bearing measurements is shown in Algorithm 1. For the bearing-based formation, Definition 2 becomes

Definition 3 *A bearing-based leader-follower formation $(\mathcal{G}, p)$ is said to be localizable if the block matrix $\mathcal{B}_{ff}$ in (15) is nonsingular, i.e., the positions of the follower group p_f can be uniquely determined by those of the leader group p_l based on inter-agent bearings.*

4 Bearing-based Distributed Localization and Formation Tracking Control

To achieve distributed localization, the localizable condition of bearing-based multi-agent systems needs to be explored. That is, how to guarantee the block matrix $\mathcal{B}_{ff}$ in (15) to be nonsingular. From Section 2.2 and (3),

Algorithm 1 Construction of Weight-matrix-based Position Constraint Using Bearing Measurements

Available information: bearing measurements among each follower i and its neighbors $j, k \in \mathcal{N}_i$;
For follower $i = m+1 : n$
  If agents i, j, k ($j, k \in \mathcal{N}_i$) are non-collinear **do**
    Based on bearing measurements, calculate H_{ij},
    H_{ik} through Algorithm 2 and Algorithm 3;
  Else, do
    The weight matrices are set to $H_{ij} = \mathbf{0}, H_{ik} = \mathbf{0}$;
  End
End
Aggregating the position constraint of each follower i into a block matrix form (13);
Obtaining the position relationship (15) between p_l and p_f.

the block matrix $\mathcal{B}_{ff}$ in (15) with our designed directed graph topology $\mathcal{G}$ is

$$\mathcal{B}_{ff} = \begin{bmatrix} H_{(m+1)(m+1)} & & & 0 \\ -H_{(m+2)(m+1)} & H_{(m+2)(m+2)} & & \\ \vdots & \vdots & \ddots & \\ -H_{n(m+1)} & -H_{n(m+2)} & \cdots & H_{nn} \end{bmatrix}. \tag{16}$$

4.1 Localizability of Bearing-based Multi-agent System

Theorem 4.1 *A bearing-based formation $(\mathcal{G}, p)$ with a directed graph topology is localizable if each follower $i \in \mathcal{V}_f$ and its neighbors are not all collinear.*

Proof. As shown in (ii) of Section 3.2, if each follower $i \in \mathcal{V}_f$ and its neighbors $j, k \in \mathcal{N}_i$ are non-collinear, the weight matrices H_{ij}, H_{ik} of agents i, j, k in (6) can be calculated based on inter-agent bearings through Algorithm 2 and Algorithm 3. Since agents i, j, k are non-collinear, agents i, j, k are not collocated. From Lemma 3.1 and (16), for the diagonal submatrices $H_{ii}, i = m+1, \cdots, n$, it has

$$\det(H_{ii}) \neq 0,\ i = m+1, \cdots, n. \tag{17}$$

Thus, it has

$$\det(\mathcal{B}_{ff}) = \prod_{i=m+1}^{n} \det(H_{ii}) \neq 0. \tag{18}$$

Hence, the block matrix $\mathcal{B}_{ff}$ in (15) is nonsingular. That is, the bearing-based formation $(\mathcal{G}, p)$ is localizable. □

In this article, the bearing-based formation $(\mathcal{G}, p)$ is not assumed to be localizable at all times shown in the following section.

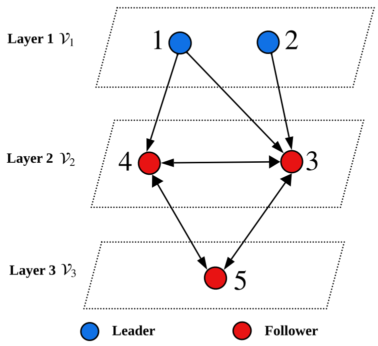

Fig. 4. An induced graph of $\mathcal{G}$ in Fig. 1.

4.2 Bearing-based Distributed Protocol

Definition 4 *The graph $\bar{\mathcal{G}}=(\mathcal{V},\bar{\mathcal{E}})$ is an induced graph of $\mathcal{G}=(\mathcal{V},\mathcal{E})$ with induced edge set $\bar{\mathcal{E}}=\mathcal{E}\cup\tilde{\mathcal{E}}$, where $\tilde{\mathcal{E}}=\{(j,i):(i,j)\in\mathcal{E}, i,j\in\mathcal{V}_f\}$ is the augmented edge set.*

The induced graph $\bar{\mathcal{G}}$ (such as Fig. 4) is obtained by making the directed edges among the followers in the graph $\mathcal{G}$ (such as Fig. 1) undirected.

Assumption 1 *The target position $p_i^*(t)$ of each agent i is first-order differentiable. The relative measurements are available. Each leader $i\in\mathcal{V}_l$ can access its position and is located at its target position. Each follower $i\in\mathcal{V}_f$ can access the target position $p_i^*(t)$ and its derivative $\dot{p}_i^*(t)$, where the target bearings $g_{ij}^*, g_{ik}^*, j,k\in\mathcal{N}_i$ are not parallel. The initial positions of the followers are within a known bounded area.*

Remark 3 *The case that each follower $i\in\mathcal{V}_f$ has no access to the target position $p_i^*(t)$ and its derivative $\dot{p}_i^*(t)$ can be solved by employing a parameter passing technique (Chen et al., 2022). Compared to our recent hybrid control design in (Fang et al., 2024), the proposed method has no dwell time or Zeno behavior problem and can have fewer neighbors and communication.*

From Theorem 4.1, a bearing-based multi-agent system $(\mathcal{G},p)$ is localizable if each follower $i\in\mathcal{V}_f$ and its neighbors $j,k\in\mathcal{N}_i$ are non-collinear. Considering that it is impractical to assume that each follower $i\in\mathcal{V}_f$ and its neighbors $j,k\in\mathcal{N}_i$ are non-collinear at all times. Inspired by (Trinh et al., 2018) and our previous work (Chen et al., 2022), we present a distributed protocol with an induced graph $\bar{\mathcal{G}}=(\mathcal{V},\bar{\mathcal{E}})$ to drive each follower $i\in\mathcal{V}_f$ out of the undesired collinear (unlocalizable) positions and get it to its target position, i.e.,

$$\begin{cases} u_i = -w(\hat{p}_i-p_i^*)+\dot{p}_i^*-\tau_i(\mathrm{sign}(\hat{p}_i-p_i^*)-\lambda_i), \\ \dot{\hat{p}}_i = -2w(\hat{p}_i-p_i^*)+\dot{p}_i^*+\sum\limits_{j,k\in\mathcal{N}_i}\xi_{ijk}+\sum\limits_{i,g\in\mathcal{N}_s,s\in\mathcal{V}_f}\xi_{sig} \\ \qquad -2\tau_i(\mathrm{sign}(\hat{p}_i-p_i^*)-\lambda_i), \end{cases} \tag{19}$$

where $w\in\mathbb{R}^+$ and $\mathrm{sign}(\cdot)$ is the signum function defined component-wise. $\tau_i=\sum\limits_{j,k\in\mathcal{N}_i}(\|g_{ij}-g_{ij}^*\|_2+\|g_{ik}-g_{ik}^*\|_2)\geq 0$. $\lambda_i\in\mathbb{R}^3$ is a non-zero adjustment term with $0<\|\lambda_i\|_2<1$. The neighbor set of each follower is defined in (3) with a directed graph $\mathcal{G}$, and

$$\begin{aligned} \xi_{ijk} &= H_{ii}^T H_{ij}(\hat{p}_j-\hat{p}_i)+H_{ii}^T H_{ik}(\hat{p}_k-\hat{p}_i), \\ \xi_{sig} &= H_{si}^T H_{ss}(\hat{p}_s-\hat{p}_i)-H_{si}^T H_{sg}(\hat{p}_g-\hat{p}_i). \end{aligned} \tag{20}$$

Remark 4 *The variable τ_i can also be designed as $\tau_i=(1-sign(\|H_{ii}\|_1))\sum\limits_{j,k\in\mathcal{N}_i}(\|g_{ij}-g_{ij}^*\|_2+\|g_{ik}-g_{ik}^*\|_2)\geq 0$. We can deduce that $\tau_i=0$ if follower i is localizable.*

Remark 5 *The weight matrices $H_{ii},H_{ij},H_{ik},H_{ss},H_{si}$, H_{sg} can be obtained by bearing measurements as shown in Section 3.2. Although the neighbor set of each follower i is defined in (3) with a directed graph $\mathcal{G}$, the proposed distributed protocol (19) is implemented in an induced graph $\bar{\mathcal{G}}$ as shown in Definition 4. For each follower $i\in\mathcal{V}_f$, the information ξ_{ijk} is obtained based on bearings along with communication with its neighbors $j,k\in\mathcal{N}_i$ through the edges in $\mathcal{E}$, while the information ξ_{sig} is obtained based on communication with follower s through the augmented edges in $\tilde{\mathcal{E}}$, where $i,g\in\mathcal{N}_s$.*

Remark 6 *The idea is that the position estimator provides position information for the controller, while the controller helps ensure that the system is localizable. The adjustment term λ_i is any bounded three-dimensional vector satisfying $0<\|\lambda_i\|_2<1$. For example, λ_i can be designed as $\lambda_i=\frac{1}{2}[\sin(\tau_i),\cos(\tau_i),\tanh(\tau_i)]^T$, where* $\tanh(\cdot)$ *is the hyperbolic tangent function.*

Let $\bar{e}_f=p_f-p_f^*\in\mathbb{R}^{3(n-m)}$ be the tracking errors of the follower group. Let $\hat{e}_f=\hat{p}_f-p_f\in\mathbb{R}^{3(n-m)}$ be the position estimation errors of the follower group. Denote by $\psi_i=-\tau_i(\mathrm{sign}(\hat{p}_i-p_i^*)-\lambda_i)$. Note that (19) can then be rewritten in a compact form as

$$\begin{cases} \dot{p}_f = -w(\hat{p}_f-p_f^*)+\dot{p}_f^*+\psi_f, \\ \dot{\hat{p}}_f = -2w(\hat{p}_f-p_f^*)+\dot{p}_f^*-\mathcal{D}_{ff}\hat{p}_f-\mathcal{D}_{fl}p_l+2\psi_f, \end{cases} \tag{21}$$

where $\psi_f=[\psi_{m+1}^T,\cdots,\psi_n^T]^T$ and

$$\mathcal{D}_{ff}=\mathcal{B}_{ff}^T\mathcal{B}_{ff},\ \mathcal{D}_{fl}=\mathcal{B}_{ff}^T\mathcal{B}_{fl}. \tag{22}$$

The block matrices $\mathcal{B}_{ff}, \mathcal{B}_{fl}$ in (22) are from (15). We get from (15) that $\mathcal{D}_{ff}\hat{p}_f + \mathcal{D}_{fl}p_l = \mathcal{D}_{ff}\hat{e}_f$. Then, (22) becomes

$$\begin{bmatrix} \dot{\bar{e}}_f \\ \dot{\hat{e}}_f \end{bmatrix} = -\begin{bmatrix} wI_{3(n-m)} & wI_{3(n-m)} \\ wI_{3(n-m)} & wI_{3(n-m)} + \mathcal{D}_{ff} \end{bmatrix} \begin{bmatrix} \bar{e}_f \\ \hat{e}_f \end{bmatrix} + \begin{bmatrix} \psi_f \\ \psi_f \end{bmatrix}. \tag{23}$$

Under Assumption 1, the initial positions of the followers are within a known bounded area, i.e., the upper bound $\|[\bar{e}_f^T(0), \hat{e}_f^T(0)]\|_2$ is known for the implementation of the distributed protocol. Let ϱ_f be the upper bound of $\|[\bar{e}_f^T(0), \hat{e}_f^T(0)]\|_2$ as

$$\varrho_f \geq \|[\bar{e}_f^T(0), \hat{e}_f^T(0)]\|_2. \tag{24}$$

Define the parameter $\phi_i \in \mathbb{R}$ of each agent i as

$$\phi_i = \begin{cases} 0, & i \in \mathcal{V}_l, \\ \varrho_f, & i \in \mathcal{V}_f. \end{cases} \tag{25}$$

Theorem 4.2 *Under Assumption 1, the bearing-based simultaneous distributed localization and formation tracking control protocol* (19) *with an induced graph $\bar{\mathcal{G}}$ can avoid inter-agent collision and achieve the localization and control objective* (5) *if for any $i, j \in \mathcal{V}$, the following two conditions hold:*

(i) $\|p_i(0) - p_j(0)\|_2 \neq 0$;
(ii) $\|p_i^*(t) - p_j^*(t)\|_2 > \phi_i + \phi_j$, *where ϕ_i, ϕ_j are given in* (25).

Remark 7 *The two conditions (i)-(ii) are used for inter-agent collision avoidance. The condition (ii) can be satisfied by tuning the target positions $p_i^*(t)$ and $p_j^*(t)$. Based on the conditions (i)-(ii), the proposed distributed protocol in* (19) *will achieve semi-global stability (Teel, 1995). In addition, if the initial positions of all followers are available, the initial position estimates and initial target positions of the followers can be set to $\hat{p}_f(0) = p_f(0) = p_f^*(0)$, and then ϱ_f in* (24) *can be set to zero.*

Proof. For the discontinuous controller (19), the Filippov solutions of (19) exist as the signum function $\text{sign}(\cdot)$ is measurable and locally essentially bounded (Filippov, 2013). For the Lyapunov function candidate $V_1 = \frac{1}{2}(\bar{e}_f^T\bar{e}_f + \hat{e}_f^T\hat{e}_f)$, $\dot{V}_1$ exists almost everywhere, i.e.,

$$\dot{V}_1 \in^{a.e.} \dot{\tilde{V}}_1, \tag{26}$$

where $a.e.$ represents "almost everywhere" and $\dot{\tilde{V}}_1$ is the set-valued Lie derivative of V_1 (Fischer et al., 2013), i.e.,

$$\begin{aligned} \dot{\tilde{V}}_1 = & -\begin{bmatrix} \bar{e}_f^T & \hat{e}_f^T \end{bmatrix} \begin{bmatrix} wI_{3(n-m)} & wI_{3(n-m)} \\ wI_{3(n-m)} & wI_{3(n-m)} + \mathcal{D}_{ff} \end{bmatrix} \begin{bmatrix} \bar{e}_f \\ \hat{e}_f \end{bmatrix} \\ & - \sum_{i=m+1}^{n} \tau_i (\hat{p}_i - p_i^*)^T (\mathcal{K}[\text{sign}(\hat{p}_i - p_i^*)] - \lambda_i) \\ = & -w\|\bar{e}_f + \hat{e}_f\|_2^2 - \hat{e}_f^T\mathcal{D}_{ff}\hat{e}_f \\ & - \sum_{i=m+1}^{n} \tau_i (\|\hat{p}_i - p_i^*\|_1 - (\hat{p}_i - p_i^*)^T\lambda_i), \end{aligned} \tag{27}$$

where $\mathcal{K}[\cdot]$ is a Filippov set-valued mapping function. We have used the fact that $x^T\mathcal{K}[\text{sign}(x)] = \{|x|\}$ to obtain the last equality of (27). Thus, $\dot{\tilde{V}}_1$ is singleton and $\dot{V}_1 = \dot{\tilde{V}}_1$. Then, (27) becomes

$$\begin{aligned} \dot{\tilde{V}}_1 & \leq -w\|\bar{e}_f + \hat{e}_f\|_2^2 - \hat{e}_f^T\mathcal{D}_{ff}\hat{e}_f - \sum_{i=m+1}^{n} \tau_i (1 - \|\lambda_i\|_2)\|\hat{p}_i - p_i^*\|_1 \\ & \leq 0. \end{aligned} \tag{28}$$

We get from (28) that

$$\|[\bar{e}_f^T(t), \hat{e}_f^T(t)]\|_2 \leq \|[\bar{e}_f^T(0), \hat{e}_f^T(0)]\|_2, \ t \geq 0. \tag{29}$$

Under Assumption 1, we get from (25) and (29) that

$$\|p_i(t) - p_i^*(t)\|_2 \leq \phi_i. \tag{30}$$

For any $i, j \in \mathcal{V}$ and $t \geq 0$, it has

$$\begin{aligned} & \|p_i(t) - p_j(t)\|_2 \\ & \geq \|p_i^*(t) - p_j^*(t)\|_2 - \|p_i(t) - p_i^*(t)\|_2 - \|p_j(t) - p_j^*(t)\|_2 \\ & \geq \|p_i^*(t) - p_j^*(t)\|_2 - \phi_i - \phi_j > 0. \end{aligned} \tag{31}$$

Hence, there will be no inter-agent collision if $\dot{\tilde{V}}_1 \leq 0$. Note that $\dot{\tilde{V}}_1 = 0$ if and only if

$$\mathcal{D}_{ff}\hat{e}_f = \mathbf{0}, \ \ \hat{p}_f = p_f^*. \tag{32}$$

Equation (32) is equivalent to

$$\mathcal{D}_{ff}\hat{e}_f = \mathbf{0}, \ \ \hat{e}_f + \bar{e}_f = \mathbf{0}. \tag{33}$$

Based on (23) and (33), it has

$$\dot{\hat{e}}_f + \dot{\bar{e}}_f = -[\tau_{m+1}\lambda_{m+1}^T, \tau_{m+2}\lambda_{m+2}^T, \cdots, \tau_n\lambda_n^T]^T. \tag{34}$$

If $\hat{e}_f \neq \mathbf{0}$, the block matrix $\mathcal{D}_{ff}$ in (32) is singular and there is at least one follower $i \in \mathcal{V}_f$ that is unlocalizable, i.e., the term $\tau_i > 0$ in (19) is positive. Since the time-varying adjustment term λ_i in (19) is designed to be nonzero, it has $\tau_i \lambda_i \neq 0$. Then, it is clear from (34) that $\dot{\hat{e}}_f + \dot{\bar{e}}_f \neq \mathbf{0}$, which implies that $\hat{e}_f + \bar{e}_f = \mathbf{0}$ in (33) cannot hold for all times. Hence, the configuration corresponding to $\hat{e}_f \neq \mathbf{0}, \hat{e}_f + \bar{e}_f = \mathbf{0}$ is not an equilibrium of (23) due to the nonzero adjustment term λ_i. From the nonsmooth corollaries of the LaSalle-Yoshizawa Theorem (Fischer et al., 2013), the follower group converges to $\hat{e}_f = \mathbf{0}, \hat{e}_f + \bar{e}_f = \mathbf{0}$, i.e., the localization and control objective $\hat{e}_f = \mathbf{0}, \bar{e}_f = \mathbf{0}$ (5) is achieved. □

Remark 8 *If the adjustment term λ_i is designed to be zero, we can know from (34) that the configuration corresponding to $\hat{e}_f \neq \mathbf{0}, \hat{e}_f + \bar{e}_f = \mathbf{0}$ is also an equilibrium of (23). For this case, if the followers are unlocalizable, they will keep unlocalizable. Note that the unlocalizable positions of the followers are not the equilibrium of (23). From the nonsmooth corollaries of the LaSalle-Yoshizawa Theorem (Fischer et al., 2013), the followers will converge to the equilibrium of (19), i.e., the followers will not go back to the unlocalizable positions.*

4.3 Bearing-ratio-of-distance-based Distributed Protocol

To design a continuous controller, the strategy is to combine bearing and ratio-of-distance measurements that are available by low-cost onboard vision (camera) sensors (Mehdifar et al., 2022). In bearing-based localization, agent i cannot be localized by agents j, k if agents i, j, k are not collocated but collinear. Compared with bearing-based localization, one remarkable advantage of bearing-ratio-of-distance-based localization is that the translation-scaling similar configuration of agents i, j, k can be obtained even if agents i, j, k are not collocated but collinear as shown in Appendix-D. That is, agent i can be localized by agents j, k at all times if agents i, j, k are not collocated. Then, Assumption 1 is relaxed as

Assumption 2 *The target position $p_i^*(t)$ of each agent i is first-order differentiable. Each leader $i \in \mathcal{V}_l$ can access its position and located at its target position. Each follower $i \in \mathcal{V}_f$ can access the target position $p_i^*(t)$ and its derivative $\dot{p}_i^*(t)$. The initial positions of the followers are within a known bounded area. The relative measurements are available.*

Based on bearing and ratio-of-distance measurements, the distributed protocol of each follower $i \in \mathcal{V}_f$ in (19) is modified as

$$\begin{cases} u_i = -w(\hat{p}_i - p_i^*) + \dot{p}_i^*, \\ \dot{\hat{p}}_i = -2w(\hat{p}_i - p_i^*) + \dot{p}_i^* + \sum\limits_{j,k \in \mathcal{N}_i} \xi_{ijk} + \sum\limits_{i,g \in \mathcal{N}_s, s \in \mathcal{V}_f} \xi_{sig}, \end{cases} \tag{35}$$

where the terms ξ_{ijk} and ξ_{sig} are given in (20). The ratio-of-distances and bearings are used to find translation-scaling similar configuration shown in Appendix-D. The weight matrices in (20) are then calculated by the translation-scaling similar configuration through Algorithm 2. (35) can be rewritten in a compact form as

$$\begin{cases} \dot{p}_f = -w(\bar{e}_f + \hat{e}_f) + \dot{p}_f^*, \\ \dot{\hat{p}}_f = -2w(\bar{e}_f + \hat{e}_f) + \dot{p}_f^* - \mathcal{D}_{ff}\hat{p}_f - \mathcal{D}_{fl}p_l, \end{cases} \tag{36}$$

where

$$\mathcal{D}_{ff} = \mathcal{B}_{ff}^T \mathcal{B}_{ff}, \; \mathcal{D}_{fl} = \mathcal{B}_{ff}^T \mathcal{B}_{fl}. \tag{37}$$

Theorem 4.3 *Under Assumption 2, the bearing-ratio-of-distance-based simultaneous distributed localization and formation tracking control protocol (35) with an induced graph $\bar{\mathcal{G}}$ can avoid inter-agent collision and achieve the localization and control objective (5) if for any $i, j \in \mathcal{V}$, the following two conditions hold:*

(i) $\|p_i(0) - p_j(0)\|_2 \neq 0$;
(ii) $\|p_i^*(t) - p_j^*(t)\|_2 > \phi_i + \phi_j$, *where ϕ_i, ϕ_j are given in (25).*

Proof. Consider a Lyapunov function candidate $V_1 = \frac{1}{2}(\bar{e}_f^T \bar{e}_f + \hat{e}_f^T \hat{e}_f)$. We have

$$\dot{V}_1 = -\begin{bmatrix} \bar{e}_f^T & \hat{e}_f^T \end{bmatrix} \begin{bmatrix} wI_{3(n-m)} & wI_{3(n-m)} \\ wI_{3(n-m)} & wI_{3(n-m)} + \mathcal{D}_{ff} \end{bmatrix} \begin{bmatrix} \bar{e}_f \\ \hat{e}_f \end{bmatrix} \leq 0. \tag{38}$$

Similar to the Proof of Theorem 4.2, we can know that there will be no inter-agent collision if $\dot{V}_1 \leq 0$. We can know from Appendix-D that the translation-scaling similar configuration can be calculated based on bearing and ratio-of-distance measurements at all times. Then, from Lemma 3.2, the weight matrices in (6) can be calculated based on the translation-scaling similar configuration through Algorithm 2 at all times. From Lemma 3.1 and (16), we can deduce that the block matrix $\mathcal{B}_{ff}$ is thus nonsingular at all times, i.e., the block matrix $\mathcal{D}_{ff} = \mathcal{B}_{ff}^T \mathcal{B}_{ff} > 0$ is positive definite for all times $t \geq 0$. Equation (38) becomes

$$\dot{V}_1 < 0, \text{ if } \; \bar{e}_f, \hat{e}_f \neq \mathbf{0}. \tag{39}$$

Hence, the objective $\hat{e}_f = \mathbf{0}, \bar{e}_f = \mathbf{0}$ (5) is achieved. □

4.4 Discussion on Other Types of Relative Measurements and Applications in 2-D Plane

The bearings or ratio-of-distances are used in the proposed distributed protocol as shown in Section 4.2 and

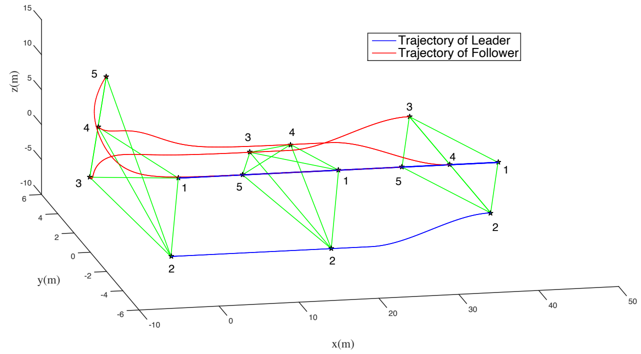

Fig. 5. Trajectories of the agents in case (i).

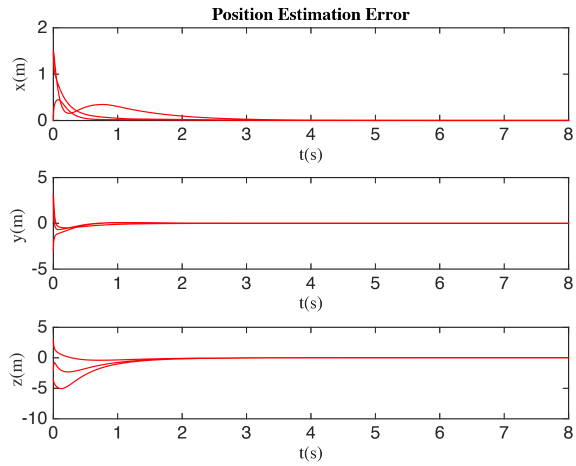

Fig. 6. Position estimation errors in case (i).

Section 4.3. Note that the bearings or ratio-of-distances among each follower i and its neighbors $j, k \in \mathcal{N}_i$ can also be obtained indirectly by relative position, distance, and angle measurements shown as follows: (i) If the relative positions p_{ij}, p_{ik} are available, the bearings g_{ij}, g_{ik} and ratio-of-distance r_{ijk} can be obtained by (2); (ii) If the distances $\|p_{ij}\|_2, \|p_{ik}\|$ are available, the ratio-of-distance r_{ijk} can be obtained by (2); (iii) If the angles θ_j, θ_k are available and agents i, j, k are non-collinear, the ratio-of-distance r_{ijk} can be obtained by $r_{ijk} = \frac{\sin\theta_k}{\sin\theta_j}$. If agents i, j, k are collinear, i.e., the ratio-of-distance r_{ijk} cannot be obtained by the angles θ_j, θ_k, the weight matrices in (6) are set to $H_{ij} = H_{ik} = \mathbf{0}$. For this situation, the idea and technique in Section 4.2 can be utilized to drive the agents out of the undesired collinear (unlocalizable) positions. Hence, the proposed method is also applicable to homogeneous or heterogeneous relative position, distance, and angle measurements.

In addition, if agents i, j, k are not collocated in 2-D plane, based on the method in Lemma 6.1, the 2-D weight matrices $H_{ij}, H_{ik} \in \mathbb{R}^{2\times 2}$ in (6) have the following form: $H_{ij} = \begin{bmatrix} c_1 & c_3 \\ -c_3 & c_1 \end{bmatrix}$ and $H_{ik} = \begin{bmatrix} c_2 & c_4 \\ -c_4 & c_2 \end{bmatrix}$, where $c_1, c_2, c_3, c_4 \in \mathbb{R}$ in (41) are calculated based on the 2-D positions p_i, p_j, p_k. It can be verified that the 2-D weight-matrix-based position constraint in (6) is invariant to translation, rotation, and scaling of p_i, p_j, p_k. Hence, the 2-D weight matrices H_{ij}, H_{ik} can be calculated based on local bearings or ratio-of-distances through Algorithms 1-3. Since the local bearings or ratio-of-distances can also be obtained indirectly by local relative position, distance, and angle measurements, the proposed weight-matrix-based position constraint is also applicable to 2-D homogeneous or heterogeneous local relative position, distance, and angle measurements.

4.5 Discussion on the Occlusions in the Environment

If the relative measurements (such as bearings or ratio-of-distances) among agents i, j, k are unavailable due to the occlusions in the environment, the weight matrices H_{ij}, H_{ik} in (6) are set as $H_{ij} = \mathbf{0}$, $H_{ik} = \mathbf{0}$ and the term τ_i in (19) is set as any positive real number. Then, D_{ff} in (23) (or (38)) will be nonsingular and $\dot{\bar{V}}_1 \leq 0$ (or $\dot{V}_1 \leq 0$). Thus, the sum of the squares of the estimation and tracking errors of the followers will not increase when there are occlusions in the environment, i.e., the proposed controller is robust to the occlusions in the environment. If the occlusions does not occur at all times, the localization and control objective can still be achieved under the proposed distributed protocol.

4.6 Comparison with Existing Works

The comparison with most related bearing-based distributed localization and formation control (Zhao et al., 2019; Tang et al., 2020, 2021; Trinh et al., 2018; Tang and Loría, 2022; Van Tran et al., 2018b; Zhu et al., 2023; Su et al., 2023; Yang et al., 2021) is given below.

(i) The application scenarios are different. The works (Zhao et al., 2019; Tang et al., 2020, 2021; Trinh et al., 2018; Tang and Loría, 2022; Van Tran et al., 2018b; Zhu et al., 2023; Su et al., 2023; Yang et al., 2021) are only applicable to bearing measurements, whereas this article provides a general distributed localization and control framework, which can accommodate different relative measurements. The bearing measurement is a special case in this article.

(ii) The requirements on the desired bearings or desired formations are different. The works (Zhu et al., 2023; Su et al., 2023; Yang et al., 2021; Tang and Loría, 2022; Tang et al., 2020, 2021) require the desired bearings or desired formations are persistently exciting. In this work, the requirement on the persistently exciting motions can be removed.

(iii) The requirements on the actual bearings are different. The controllers in (Zhao et al., 2019; Tang

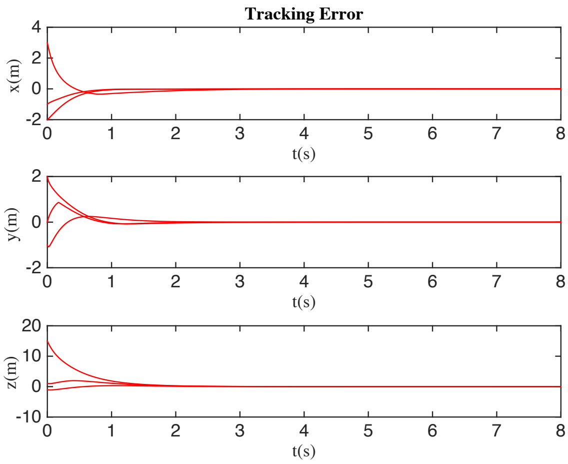

Fig. 7. Tracking errors in case (i).

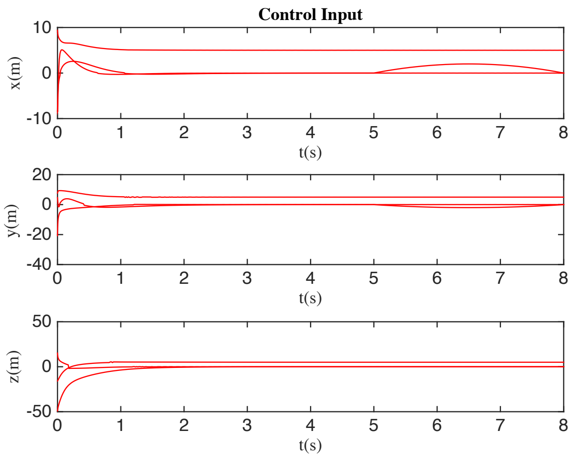

Fig. 8. Control inputs in case (i).

et al., 2020, 2021; Trinh et al., 2018; Tang and Loría, 2022; Van Tran et al., 2018b; Zhu et al., 2023; Su et al., 2023; Yang et al., 2021) require that the actual bearings are measurable at all times. In our work, the proposed method can still work if the actual bearings are not measurable. For this case, the sum of the squares of the estimation and tracking errors of the followers will not increase. That is, the proposed controller is robust to the occlusions in the environment.

(iv) The coordinate frames are different in 2-D plane. The bearing measurements in (Trinh et al., 2018; Tang et al., 2020, 2021; Zhao et al., 2019; Van Tran et al., 2018b; Tang and Loría, 2022; Su et al., 2023; Yang et al., 2021) are measured in the global coordinate frame, whereas the proposed weight-matrix-based position constraint can not only be calculated by 2-D local bearing measurements, but also by other types of 2-D homogeneous or heterogeneous local relative measurements.

(v) The implementation conditions are different. The works in (Tang et al., 2020; Yang et al., 2021; Tang et al., 2021) require that there is no inter-agent collision among the agents, whereas the proposed controller can guarantee inter-agent collision avoidance. The work in (Su et al., 2023; Tang et al., 2021; Zhu et al., 2023; Yang et al., 2021; Van Tran et al., 2018b) needs additional relative velocities, relative orientations, velocity information of the leaders, or derivatives of bearings, which is not required in this work. The works (Su et al., 2023; Zhu et al., 2023; Yang et al., 2021; Zhao and Zelazo, 2016) are only applicable to 2-D plane or static agents, whereas the proposed method is applicable to both 2-D and 3-D dynamic agents.

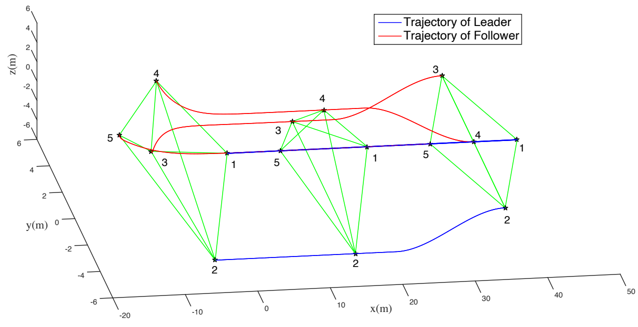

Fig. 9. Trajectories of the agents in case (ii).

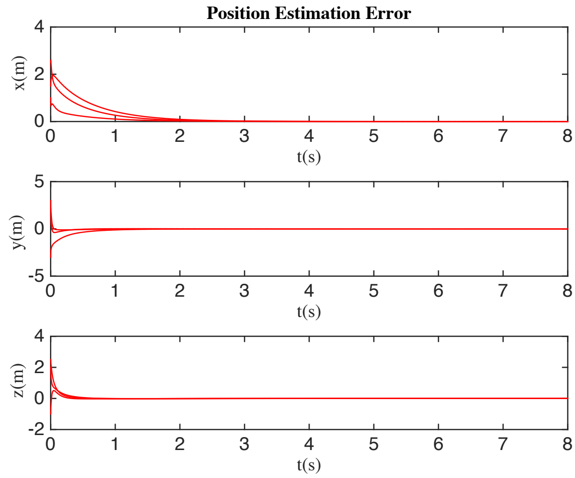

Fig. 10. Position estimation errors in case (ii).

5 Simulation

In this section, we present two simulation examples in 3-D space, where the formations consist of 2 leaders $\mathcal{V}_l = \{1, 2\}$ and 3 followers $\mathcal{V}_f = \{3, 4, 5\}$. The graph $\mathcal{G}$ of the following case (i) and case (ii) is given in Fig. 1. The induced graph $\bar{\mathcal{G}}$ for implementing the proposed distributed protocol (19) or (35) is given in Fig. 4.

Case (i): If only the bearing measurements are available,

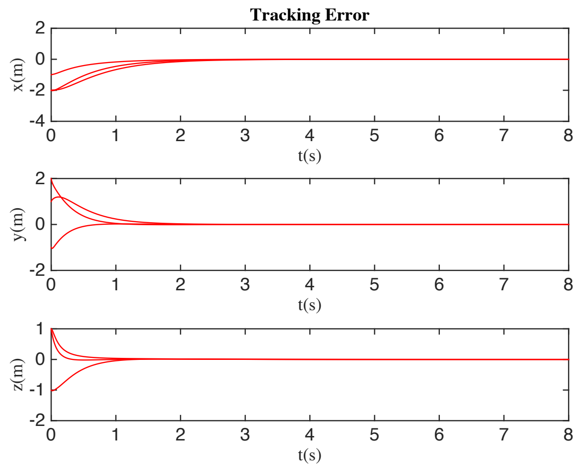

Fig. 11. Tracking errors in case (ii).

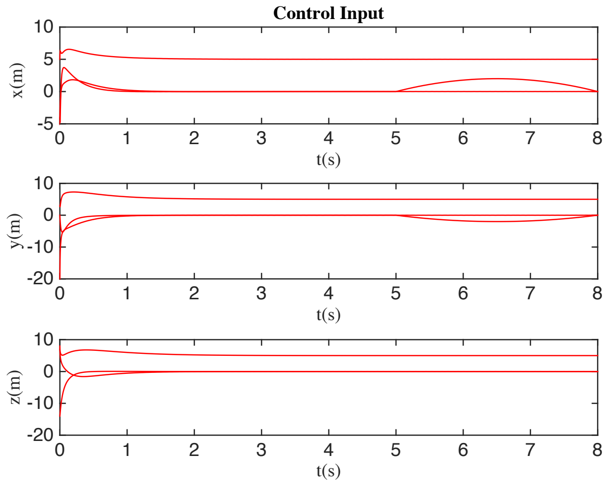

Fig. 12. Control inputs in case (ii).

the followers can achieve the objective (5) under the proposed bearing-based distributed protocol (19). The positions of the followers $3,4,5$ are collinear at some time instants as shown in Fig. 5, where the adjustment term λ_i in bearing-based distributed protocol (19) can drive the followers out of undesired collinear (unlocalizable) condition and get to their target positions. The position estimation errors and formation tracking errors converge to zero as shown in Fig. 6 and Fig. 7, respectively. The control inputs are given in Fig. 8.

Case (ii): If the bearing and ratio-of-distance measurements are available, the followers can achieve self-localization and form time-varying target formation under the bearing-ratio-of-distance-based distributed protocol (35), where there is no inter-agent collision among the agents as shown in Fig. 9. We can know from Fig. 10 and Fig. 11 that both the position estimation errors and formation tracking errors converge to zero. The corresponding control inputs are given in Fig. 12.

6 Conclusion

This paper addresses the problem of 3-D relative-measurement-based simultaneous distributed localization and formation tracking control. Two simultaneous distributed localization and formation tracking control protocols are proposed for the followers to achieve self-localization and track their target positions asymptotically, while the inter-agent collision is avoided under some conditions. A remarkable advantage is that the proposed method can be implemented without persistently exciting motions.

The limitation of the proposed approach is that the global coordinate frame is needed in 3-D space. The 3-D orientation estimation algorithm may be used to remove the requirement of global coordinate frame as in (Boughellaba and Tayebi, 2020). Future work will focus on distributed localization and formation tracking control with nonlinear agent dynamics and distance measurements. From Assumptions 1-2, we only require that the target position $p_i^*(t)$ of each agent i be first-order differentiable. There is no restriction on the transformation of target formation. Thus, the target formation can be designed based on distance rigidity. In addition, the uncertainty or disturbances could be taken into consideration as in (Su et al., 2023).

Appendix

A Calculation of the Weight Matrices H_{ij}, H_{ik}

Lemma 6.1 *Consider the 2-D vectors* $b_1 = [b_{11}, b_{12}]^T$, $b_2 = [b_{21}, b_{22}]^T$, $b_3 = [b_{31}, b_{32}]^T$. *If* $b_1 \neq b_2 \neq b_3$, *the following inequality holds:*

$$(c_1 + c_2)^2 + (c_3 + c_4)^2 \neq 0, \tag{40}$$

where

$$c_1 = \frac{b_{21}-b_{11}}{\|b_1-b_2\|_2^2},\ c_2 = \frac{b_{11}-b_{31}}{\|b_1-b_3\|_2^2},\ c_3 = \frac{b_{22}-b_{12}}{\|b_1-b_2\|_2^2},\ c_4 = \frac{b_{12}-b_{32}}{\|b_1-b_3\|_2^2}. \tag{41}$$

Proof. For the 2-D vectors $b_1, b_2, b_3 \in \mathbb{R}^2$, we have

$$\begin{bmatrix} c_1 & c_3 \\ -c_3 & c_1 \end{bmatrix}(b_2 - b_1) + \begin{bmatrix} c_2 & c_4 \\ -c_4 & c_2 \end{bmatrix}(b_3 - b_1) = \mathbf{0}. \tag{42}$$

If the inequality (40) does not hold, i.e., $c_1 = -c_2$ and $c_3 = -c_4$, (42) becomes

$$\begin{bmatrix} -c_2 & -c_4 \\ c_4 & -c_2 \end{bmatrix}(b_2 - b_1) + \begin{bmatrix} c_2 & c_4 \\ -c_4 & c_2 \end{bmatrix}(b_3 - b_1) = \mathbf{0}. \tag{43}$$

We get from (43) that $\begin{bmatrix} c_2 & c_4 \\ -c_4 & c_2 \end{bmatrix}(b_3 - b_2) = \mathbf{0}$. From (41), it has $\det(\begin{bmatrix} c_2 & c_4 \\ -c_4 & c_2 \end{bmatrix}) = \frac{1}{\|b_1-b_3\|_2^2} \neq 0$. Then, we can deduce that $b_2 = b_3$, which contradicts the fact that $b_2 \neq b_3$. Thus, the inequality (40) holds. □

A.1 Plain Position and Plain-position-based Parameters

The position of agent i in 3-D space is $p_i = [x_i, y_i, z_i]^T \in \mathbb{R}^3$. Define the plane positions of agent i as

$$\alpha_i = [x_i, y_i]^T, \quad \beta_i = [y_i, z_i]^T, \quad \gamma_i = [z_i, x_i]^T, \tag{44}$$

where $\alpha_i, \beta_i, \gamma_i \in \mathbb{R}^2$ are, respectively, the plane positions of agent i in X-Y plane, Y-Z plane, and Z-X plane. For agents j, k, their plane positions are $\alpha_j, \beta_j, \gamma_j$ and $\alpha_k, \beta_k, \gamma_k$. The plain-position-based parameters $s_1, \cdots, s_{12}$ in (45) will be used in the calculation of the weight matrices H_{ij}, H_{ik}.

$$\begin{aligned}
&s_1 = \tfrac{\tau_1(\tau_1+\tau_2)+\tau_3(\tau_3+\tau_4)}{(\tau_1+\tau_2)^2+(\tau_3+\tau_4)^2}, \quad s_2 = \tfrac{-\tau_3(\tau_1+\tau_2)+\tau_1(\tau_3+\tau_4)}{(\tau_1+\tau_2)^2+(\tau_3+\tau_4)^2}, \\
&s_3 = \tfrac{\tau_2(\tau_1+\tau_2)+\tau_4(\tau_3+\tau_4)}{(\tau_1+\tau_2)^2+(\tau_3+\tau_4)^2}, \quad s_4 = \tfrac{-\tau_4(\tau_1+\tau_2)+\tau_2(\tau_3+\tau_4)}{(\tau_1+\tau_2)^2+(\tau_3+\tau_4)^2}, \\
&s_5 = \tfrac{\tau_5(\tau_5+\tau_6)+\tau_7(\tau_7+\tau_8)}{(\tau_5+\tau_6)^2+(\tau_7+\tau_8)^2}, \quad s_6 = \tfrac{-\tau_7(\tau_5+\tau_6)+\tau_5(\tau_7+\tau_8)}{(\tau_5+\tau_6)^2+(\tau_7+\tau_8)^2}, \\
&s_7 = \tfrac{\tau_6(\tau_5+\tau_6)+\tau_8(\tau_7+\tau_8)}{(\tau_5+\tau_6)^2+(\tau_7+\tau_8)^2}, \quad s_8 = \tfrac{-\tau_8(\tau_5+\tau_6)+\tau_6(\tau_7+\tau_8)}{(\tau_5+\tau_6)^2+(\tau_7+\tau_8)^2}, \\
&s_9 = \tfrac{\tau_9(\tau_9+\tau_{10})+\tau_{11}(\tau_{11}+\tau_{12})}{(\tau_9+\tau_{10})^2+(\tau_{11}+\tau_{12})^2}, \quad s_{10} = \tfrac{-\tau_{11}(\tau_9+\tau_{10})+\tau_9(\tau_{11}+\tau_{12})}{(\tau_9+\tau_{10})^2+(\tau_{11}+\tau_{12})^2}, \\
&s_{11} = \tfrac{\tau_{10}(\tau_9+\tau_{10})+\tau_{12}(\tau_{11}+\tau_{12})}{(\tau_9+\tau_{10})^2+(\tau_{11}+\tau_{12})^2}, s_{12} = \tfrac{-\tau_{12}(\tau_9+\tau_{10})+\tau_{10}(\tau_{11}+\tau_{12})}{(\tau_9+\tau_{10})^2+(\tau_{11}+\tau_{12})^2},
\end{aligned} \tag{45}$$

where

$$\begin{aligned}
&\tau_1 = \tfrac{x_j-x_i}{\|\alpha_i-\alpha_j\|_2^2}, \tau_2 = \tfrac{x_i-x_k}{\|\alpha_i-\alpha_k\|_2^2}, \tau_3 = \tfrac{y_j-y_i}{\|\alpha_i-\alpha_j\|_2^2}, \tau_4 = \tfrac{y_i-y_k}{\|\alpha_i-\alpha_k\|_2^2}, \\
&\tau_5 = \tfrac{y_j-y_i}{\|\beta_i-\beta_j\|_2^2}, \tau_6 = \tfrac{y_i-y_k}{\|\beta_i-\beta_k\|_2^2}, \ \tau_7 = \tfrac{z_j-z_i}{\|\beta_i-\beta_j\|_2^2}, \tau_8 = \tfrac{z_i-z_k}{\|\beta_i-\beta_k\|_2^2}, \\
&\tau_9 = \tfrac{x_j-x_i}{\|\gamma_i-\gamma_j\|_2^2}, \tau_{10} = \tfrac{x_i-x_k}{\|\gamma_i-\gamma_k\|_2^2}, \tau_{11} = \tfrac{z_j-z_i}{\|\gamma_i-\gamma_j\|_2^2}, \tau_{12} = \tfrac{z_i-z_k}{\|\gamma_i-\gamma_k\|_2^2}.
\end{aligned} \tag{46}$$

A.2 Calculation of Weight Matrices H_{ij}, H_{ik} Based on Plain Position

If follower $i \in \mathcal{V}_f$ and its two neighbors $j, k \in \mathcal{N}_i$ are not collocated, i.e., $p_i \neq p_j \neq p_k$, there are four cases for the plain positions $\alpha_i, \alpha_j, \alpha_k$: (1) $\alpha_i \neq \alpha_j \neq \alpha_k$; (2) $\alpha_i = \alpha_j$; (3) $\alpha_i \neq \alpha_j, \alpha_i = \alpha_k$; (4) $\alpha_i \neq \alpha_j$, $\alpha_j = \alpha_k$.

Algorithm 2 Construction of Weight Matrices H_{ij}, H_{ik} Based on Plain Position

Available information: plain positions of agents i, j, k.
If $\alpha_i \neq \alpha_j \neq \alpha_k$ **do**
  Calculating H_{ij}, H_{ik} by (49)-(54);
Else if $\alpha_i = \alpha_j$ **do**
  Calculating H_{ij}, H_{ik} by (55)-(58);
Else if $\alpha_i \neq \alpha_j, \alpha_i = \alpha_k$ **do**
  Calculating H_{ij}, H_{ik} by (59)-(62);
Else, do
  Calculating H_{ij}, H_{ik} by (63)-(69);
End

Case (1): For the first case $\alpha_i \neq \alpha_j \neq \alpha_k$, it has

$$\begin{bmatrix} \tau_1 & \tau_3 \\ -\tau_3 & \tau_1 \end{bmatrix}(\alpha_j - \alpha_i) + \begin{bmatrix} \tau_2 & \tau_4 \\ -\tau_4 & \tau_2 \end{bmatrix}(\alpha_k - \alpha_i) = \mathbf{0}, \tag{47}$$

where $\tau_1, \tau_2, \tau_3, \tau_4$ are given in (46). From Lemma 6.1,

$$(\tau_1+\tau_2)^2 + (\tau_3+\tau_4)^2 \neq 0. \tag{48}$$

For case (1), there are six subcases (1.1)-(1.6) for the plane positions $\beta_i, \beta_j, \beta_k$ and $\gamma_i, \gamma_j, \gamma_k$: (1.1) $\beta_i = \beta_j$; (1.2) $\beta_i \neq \beta_j, \beta_i = \beta_k$; (1.3) $\beta_i \neq \beta_j \neq \beta_k$; (1.4) $\beta_i \neq \beta_j, \beta_j = \beta_k, \gamma_i = \gamma_j$; (1.5) $\beta_i \neq \beta_j, \beta_j = \beta_k, \gamma_i \neq \gamma_j, \gamma_i = \gamma_k$; (1.6) $\beta_i \neq \beta_j, \beta_j = \beta_k, \gamma_i \neq \gamma_j \neq \gamma_k$. Note that the subcase $\beta_i \neq \beta_j, \beta_j = \beta_k, \gamma_j = \gamma_k$ is unreasonable if agents i, j, k are not collocated. Other unreasonable subcases of case (2)-(4) will also be excluded and not discussed.

(1.1) For the first subcase of case (1), it has $\beta_i - \beta_j = \mathbf{0}$. Then, based on plain position relationship (47) and $\beta_i - \beta_j = \mathbf{0}$, we can obtain the weight matrices H_{ij}, H_{ik} in (6), i.e.,

$$H_{ij} = \begin{bmatrix} s_1 & -s_2 & 0 \\ s_2 & 1+s_1 & 0 \\ 0 & 0 & 1 \end{bmatrix}, H_{ik} = \begin{bmatrix} s_3 & -s_4 & 0 \\ s_4 & s_3 & 0 \\ 0 & 0 & 0 \end{bmatrix}, \tag{49}$$

where s_1, s_2, s_3, s_4 are defined in (45). Then, we can calculate the weight matrices H_{ij}, H_{ik} based on the plain positions of agents i, j, k for the subcases (1.2)-(1.6).

(1.2) For the second subcase of case (1), the weight matrices H_{ij}, H_{ik} are calculated as

$$H_{ij} = \begin{bmatrix} s_1 & -s_2 & 0 \\ s_2 & s_1 & 0 \\ 0 & 0 & 0 \end{bmatrix}, \ H_{ik} = \begin{bmatrix} s_3 & -s_4 & 0 \\ s_4 & 1+s_3 & 0 \\ 0 & 0 & 1 \end{bmatrix}. \tag{50}$$

(1.3) For the third subcase of case (1), the weight matrices H_{ij}, H_{ik} are calculated as

$$H_{ij}=\begin{bmatrix} s_1 & -s_2 & 0 \\ s_2 & s_1+s_5 & -s_6 \\ 0 & s_6 & s_5 \end{bmatrix}, H_{ik}=\begin{bmatrix} s_3 & -s_4 & 0 \\ s_4 & s_3+s_7 & -s_8 \\ 0 & s_8 & s_7 \end{bmatrix}, \quad (51)$$

where s_5, s_6, s_7, s_8 are defined in (45).

(1.4) For the fourth subcase of case (1), the weight matrices H_{ij}, H_{ik} are calculated as

$$H_{ij}=\begin{bmatrix} 1+s_1 & -s_2 & 0 \\ s_2 & s_1 & 0 \\ 0 & 0 & 1 \end{bmatrix}, H_{ik}=\begin{bmatrix} s_3 & -s_4 & 0 \\ s_4 & s_3 & 0 \\ 0 & 0 & 0 \end{bmatrix}. \quad (52)$$

(1.5) For the fifth subcase of case (1), the weight matrices H_{ij}, H_{ik} are calculated as

$$H_{ij}=\begin{bmatrix} s_1 & -s_2 & 0 \\ s_2 & s_1 & 0 \\ 0 & 0 & 0 \end{bmatrix}, H_{ik}=\begin{bmatrix} 1+s_3 & -s_4 & 0 \\ s_4 & s_3 & 0 \\ 0 & 0 & 1 \end{bmatrix}. \quad (53)$$

(1.6) For the sixth subcase of case (1), the weight matrices H_{ij}, H_{ik} are calculated as

$$H_{ij}=\begin{bmatrix} s_1+s_9 & -s_2 & -s_{10} \\ s_2 & s_1 & 0 \\ s_{10} & 0 & s_9 \end{bmatrix}, H_{ik}=\begin{bmatrix} s_3+s_{11} & -s_4 & -s_{12} \\ s_4 & s_3 & 0 \\ s_{12} & 0 & s_{11} \end{bmatrix}, \quad (54)$$

where $s_9, s_{10}, s_{11}, s_{12}$ are defined in (45).

Case (2): For the second case $\alpha_i=\alpha_j$, it has $\alpha_i-\alpha_j=\mathbf{0}$. If the agents i, j, k are not collocated, it has $\beta_i \neq \beta_j$ and $\gamma_i \neq \gamma_j$. There are four subcases (2.1)-(2.4) for the plane positions $\beta_i, \beta_j, \beta_k$ and $\gamma_i, \gamma_j, \gamma_k$: (2.1) $\beta_i = \beta_k$; (2.2) $\beta_i \neq \beta_j \neq \beta_k$; (2.3) $\beta_i \neq \beta_k, \beta_j = \beta_k, \gamma_i = \gamma_k$; (2.4) $\beta_i \neq \beta_k, \beta_j = \beta_k, \gamma_i \neq \gamma_j \neq \gamma_k$.

(2.1) For the first subcase of case (2), the weight matrices H_{ij}, H_{ik} are calculated as

$$H_{ij}=\begin{bmatrix} 1 & 0 & 0 \\ 0 & 1 & 0 \\ 0 & 0 & 0 \end{bmatrix}, H_{ik}=\begin{bmatrix} 0 & 0 & 0 \\ 0 & 1 & 0 \\ 0 & 0 & 1 \end{bmatrix}. \quad (55)$$

(2.2) For the second subcase of case (2), the weight matrices H_{ij}, H_{ik} are calculated as

$$H_{ij}=\begin{bmatrix} 1 & 0 & 0 \\ 0 & 1+s_5 & -s_6 \\ 0 & s_6 & s_5 \end{bmatrix}, H_{ik}=\begin{bmatrix} 0 & 0 & 0 \\ 0 & s_7 & -s_8 \\ 0 & s_8 & s_7 \end{bmatrix}. \quad (56)$$

(2.3) For the third subcase of case (2), the weight matrices H_{ij}, H_{ik} are calculated as

$$H_{ij}=\begin{bmatrix} 1 & 0 & 0 \\ 0 & 1 & 0 \\ 0 & 0 & 0 \end{bmatrix}, H_{ik}=\begin{bmatrix} 1 & 0 & 0 \\ 0 & 0 & 0 \\ 0 & 0 & 1 \end{bmatrix}. \quad (57)$$

(2.4) For the fourth subcase of case (2), the weight matrices H_{ij}, H_{ik} are calculated as

$$H_{ij}=\begin{bmatrix} 1+s_9 & 0 & -s_{10} \\ 0 & 1 & 0 \\ s_{10} & 0 & s_9 \end{bmatrix}, H_{ik}=\begin{bmatrix} s_{11} & 0 & -s_{12} \\ 0 & 0 & 0 \\ s_{12} & 0 & s_{11} \end{bmatrix}. \quad (58)$$

Case (3): For the third case $\alpha_i \neq \alpha_j, \alpha_i = \alpha_k$ of the plain positions $\alpha_i, \alpha_j, \alpha_k$, it has $\alpha_i - \alpha_k = \mathbf{0}$. If the agents i, j, k are not collocated, it has $\beta_i \neq \beta_k$ and $\gamma_i \neq \gamma_k$. There are four subcases (3.1)-(3.4) for the plane positions $\beta_i, \beta_j, \beta_k$ and $\gamma_i, \gamma_j, \gamma_k$: (3.1) $\beta_i = \beta_j$; (3.2) $\beta_i \neq \beta_j \neq \beta_k$; (3.3) $\beta_i \neq \beta_j, \beta_j = \beta_k, \gamma_i = \gamma_j$; (3.4) $\beta_i \neq \beta_j, \beta_j = \beta_k, \gamma_i \neq \gamma_j \neq \gamma_k$.

(3.1) For the first subcase of case (3), H_{ij}, H_{ik} are calculated as

$$H_{ij}=\begin{bmatrix} 0 & 0 & 0 \\ 0 & 1 & 0 \\ 0 & 0 & 1 \end{bmatrix}, H_{ik}=\begin{bmatrix} 1 & 0 & 0 \\ 0 & 1 & 0 \\ 0 & 0 & 0 \end{bmatrix}. \quad (59)$$

(3.2) For the second subcase of case (3), the weight matrices H_{ij}, H_{ik} are calculated as

$$H_{ij}=\begin{bmatrix} 0 & 0 & 0 \\ 0 & s_5 & -s_6 \\ 0 & s_6 & s_5 \end{bmatrix}, H_{ik}=\begin{bmatrix} 1 & 0 & 0 \\ 0 & 1+s_7 & -s_8 \\ 0 & s_8 & s_7 \end{bmatrix}. \quad (60)$$

(3.3) For the third subcase of case (3), the weight matrices H_{ij}, H_{ik} are calculated as

$$H_{ij}=\begin{bmatrix}1&0&0\\0&0&0\\0&0&1\end{bmatrix},\ H_{ik}=\begin{bmatrix}1&0&0\\0&1&0\\0&0&0\end{bmatrix}. \tag{61}$$

(3.4) For the fourth subcase of case (3), the weight matrices H_{ij}, H_{ik} are calculated as

$$H_{ij}=\begin{bmatrix}s_9&0&-s_{10}\\0&0&0\\s_{10}&0&s_9\end{bmatrix},\ H_{ik}=\begin{bmatrix}1+s_{11}&0&-s_{12}\\0&1&0\\s_{12}&0&s_{11}\end{bmatrix}. \tag{62}$$

Case (4): For the fourth case $\alpha_i\neq\alpha_j, \alpha_j=\alpha_k$ of the plain positions $\alpha_i, \alpha_j, \alpha_k$, it has $\beta_j\neq\beta_k$ and $\gamma_j\neq\gamma_k$ if the agents i, j, k are not collocted. There are seven subcases (4.1)-(4.7) for the plane positions $\beta_i, \beta_j, \beta_k$ and $\gamma_i, \gamma_j, \gamma_k$: (4.1) $\beta_i=\beta_j, \gamma_i=\gamma_k$; (4.2) $\beta_i=\beta_j, \gamma_i\neq\gamma_k$; (4.3) $\beta_i\neq\beta_j, \beta_i=\beta_k, \gamma_i=\gamma_j$; (4.4) $\beta_i\neq\beta_j, \beta_i=\beta_k, \gamma_i\neq\gamma_j$; (4.5) $\beta_i\neq\beta_j\neq\beta_k, \gamma_i=\gamma_j$; (4.6) $\beta_i\neq\beta_j\neq\beta_k, \gamma_i\neq\gamma_j, \gamma_i=\gamma_k$; (4.7) $\beta_i\neq\beta_j\neq\beta_k, \gamma_i\neq\gamma_j\neq\gamma_k$.

(4.1) For the first subcase of case (4), the weight matrices H_{ij}, H_{ik} are calculated as

$$H_{ij}=\begin{bmatrix}0&0&0\\0&1&0\\0&0&1\end{bmatrix},\ H_{ik}=\begin{bmatrix}1&0&0\\0&0&0\\0&0&1\end{bmatrix}. \tag{63}$$

(4.2) For the second subcase of case (4), the weight matrices H_{ij}, H_{ik} are calculated as

$$H_{ij}=\begin{bmatrix}s_9&0&-s_{10}\\0&1&0\\s_{10}&0&1+s_9\end{bmatrix},\ H_{ik}=\begin{bmatrix}s_{11}&0&-s_{12}\\0&0&0\\s_{12}&0&s_{11}\end{bmatrix}. \tag{64}$$

(4.3) For the third subcase of case (4), the weight matrices H_{ij}, H_{ik} are calculated as

$$H_{ij}=\begin{bmatrix}1&0&0\\0&0&0\\0&0&1\end{bmatrix},\ H_{ik}=\begin{bmatrix}0&0&0\\0&1&0\\0&0&1\end{bmatrix}. \tag{65}$$

(4.4) For the fourth subcase of case (4), the weight matrices H_{ij}, H_{ik} are calculated as

$$H_{ij}=\begin{bmatrix}s_9&0&-s_{10}\\0&0&0\\s_{10}&0&s_9\end{bmatrix},\ H_{ik}=\begin{bmatrix}s_{11}&0&-s_{12}\\0&1&0\\s_{12}&0&1+s_{11}\end{bmatrix}. \tag{66}$$

(4.5) For the fifth subcase of case (4), the weight matrices H_{ij}, H_{ik} are calculated as

$$H_{ij}=\begin{bmatrix}1&0&0\\0&s_5&-s_6\\0&s_6&1+s_5\end{bmatrix},\ H_{ik}=\begin{bmatrix}0&0&0\\0&s_7&-s_8\\0&s_8&s_7\end{bmatrix}. \tag{67}$$

(4.6) For the sixth subcase of case (4), the weight matrices H_{ij}, H_{ik} are calculated as

$$H_{ij}=\begin{bmatrix}0&0&0\\0&s_5&-s_6\\0&s_6&s_5\end{bmatrix},\ H_{ik}=\begin{bmatrix}1&0&0\\0&s_7&-s_8\\0&s_8&1+s_7\end{bmatrix}. \tag{68}$$

(4.7) For the seventh subcase of case (4), the weight matrices H_{ij}, H_{ik} are calculated as

$$H_{ij}=\begin{bmatrix}s_9&0&-s_{10}\\0&s_5&-s_6\\s_{10}&s_6&s_5+s_9\end{bmatrix},\ H_{ik}=\begin{bmatrix}s_{11}&0&-s_{12}\\0&s_7&-s_8\\s_{12}&s_8&s_7+s_{11}\end{bmatrix}. \tag{69}$$

B Proof of Lemma 3.1

Proof. If the agents i, j, k are not collocated, there are twenty-one subcases for the calculation of the weight matrices H_{ij}, H_{ik} as shown in Appendix-A. For the first subcase (49), we have

$$H_{ii}=H_{ij}+H_{ik}=\begin{bmatrix}s_1+s_3&-s_2-s_4&0\\s_2+s_4&1+s_1+s_3&0\\0&0&1\end{bmatrix}. \tag{70}$$

From (45), it has $s_1+s_3=1$ and $s_2+s_4=0$. Then, (70) becomes

$$H_{ii}=H_{ij}+H_{ik}=\begin{bmatrix}1&0&0\\0&2&0\\0&0&1\end{bmatrix}. \tag{71}$$

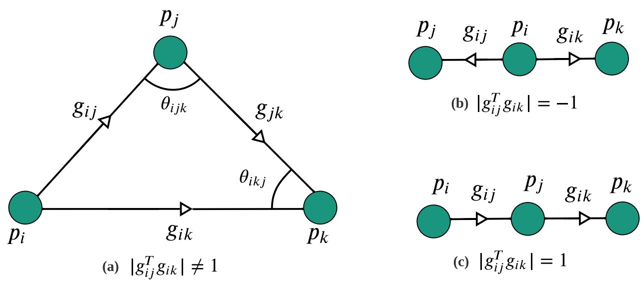

Fig. 13. Examples of the distribution of the agents i, j, k.

Hence, the matrix H_{ii} is nonsingular for the first subcase (49). By using a similar argument, it can be shown that the matrix H_{ii} is nonsingular for the rest subcases (50)-(69). $\square$

Algorithm 3 Calculation of Translation-scaling Similar Configuration

1: Available information: bearings or ratio-of-distances among agents i, j, k.
2: **If** the agents i, j, k are non-collinear and bearings are available **do**
3: $q_i = 0$, $q_j = g_{ij}$, and q_k is calculated by (74);
4: **End**
5: **If** agents i, j, k are not collocated and both bearing and ratio-of-distance measurements are available **do**
6: $q_i = 0$, $q_j = g_{ij}$, and q_k is calculated by (77);
7: **End**

C Bearing-based Translation-scaling Similar Configuration

If the agents i, j, k are non-collinear, we can obtain a translation-scaling similar configuration $\check{q} = [q_i^T, q_j^T, q_k^T]^T$ of $\check{p} = [p_i^T, p_j^T, p_k^T]^T$ based on bearing measurements shown as follows: g_{ij}, g_{ik}, and g_{jk} are the bearing measurements among the agents i, j, k. If $|g_{ij}^T g_{ik}| \neq 1$, agents i, j, k are non-collinear shown in Fig.13(a). q_i and q_j are designed satisfying $g_{ij} = \frac{q_j - q_i}{\|q_j - q_i\|_2}$. Set $q_i = [0, 0, 0]^T$ and $q_j = g_{ij}$. The distance d_{ik} between q_i and q_k can be calculated by

$$d_{ik} = \|q_j - q_i\|_2 \cdot \frac{\sin\theta_{ijk}}{\sin\theta_{ikj}} = \frac{\sin\theta_{ijk}}{\sin\theta_{ikj}}, \tag{72}$$

where the angles θ_{ijk} and θ_{ikj} are

$$\theta_{ijk} = \arccos(-g_{ij}^T g_{jk}),\ \theta_{ikj} = \arccos(g_{ik}^T g_{jk}). \tag{73}$$

From Fig.13(a), the position q_k is calculated as

$$q_k = d_{ik} g_{ik} + q_i = g_{ik} \frac{\sin(\arccos(-g_{ij}^T g_{jk}))}{\sin(\arccos(g_{ik}^T g_{jk}))}. \tag{74}$$

For the positions q_i, q_j, q_k, it has

$$\frac{q_j - q_i}{\|q_j - q_i\|_2} = g_{ij},\ \frac{q_k - q_j}{\|q_k - q_j\|_2} = g_{jk},\ \frac{q_k - q_i}{\|q_k - q_i\|_2} = g_{ik}. \tag{75}$$

Hence, the configurations $\check{q} = [q_i^T, q_j^T, q_k^T]^T$ and $\check{p} = [p_i^T, p_j^T, p_k^T]^T$ have the same inter-agent bearings, i.e., the configuration $\check{q} = [q_i^T, q_j^T, q_k^T]^T$ is a translation-scaling similar configuration of $\check{p} = [p_i^T, p_j^T, p_k^T]^T$. For example, if the positions of agents i, j, k are $p_i = [1, 0, 1]^T$, $p_j = [3, 0, 1]^T$, $p_k = [2, 2, 3]^T$, we can calculate its translation-scaling similar configuration of $\check{p} = [p_i^T, p_j^T, p_k^T]^T$ as

$$q_i = [0, 0, 0]^T,\ q_j = [1, 0, 0]^T,\ q_k = [\frac{1}{2}, 1, 1]^T. \tag{76}$$

D Bearing-ratio-of-distance-based Translation-scaling Similar Configuration

If agents i, j, k are not collocated as shown in Fig.13(a)-(c). We can combine bearing and ratio-of-distance measurements to obtain a translation-scaling similar configuration $\check{q} = [q_i^T, q_j^T, q_k^T]^T$ of $\check{p} = [p_i^T, p_j^T, p_k^T]^T$. Note that $r_{ijk} = \frac{\|p_j - p_i\|_2}{\|p_k - p_i\|_2}$ is the ratio-of-distance measurement among agents p_i, p_j, p_k. Set $q_i = [0, 0, 0]^T$ and $q_j = g_{ij}$. Then, it has

$$q_k = g_{ik} \tfrac{\|q_j - q_i\|_2}{r_{ijk}} = \tfrac{g_{ik}}{r_{ijk}}. \tag{77}$$

For example, if the positions of agents i, j, k are $p_i = [1, 0, 1]^T$, $p_j = [3, 0, 1]^T$, $p_k = [4, 0, 1]^T$, we can calculate its translation-scaling similar configuration of $\check{p} = [p_i^T, p_j^T, p_k^T]^T$ as

$$q_i = [0, 0, 0]^T,\ q_j = [1, 0, 0]^T,\ q_k = [\frac{3}{2}, 0, 0]^T. \tag{78}$$

References

Aspnes, J., Eren, T., Goldenberg, D. K., Morse, A. S., Whiteley, W., Yang, Y. R., Anderson, B. D., and Belhumeur, P. N. (2006). A theory of network localization. *IEEE Transactions on Mobile Computing*, 5(12):1663–1678.

Barooah, P. and Hespanha, J. P. (2007). Estimation on graphs from relative measurements. *IEEE Control Systems Magazine*, 27(4):57–74.

Boughellaba, M. and Tayebi, A. (2020). Distributed attitude estimation for multi-agent systems on *so*(3). *IEEE Transactions on Automatic Control*, 70(12):5696–5710.

Chen, L., Xie, L., Li, X., Fang, X., and Feroskhan, M. (2022). Simultaneous localization and formation using angle-only measurements in 2d. *Automatica*, 146:110605.

Eren, T., Goldenberg, O., Whiteley, W., Yang, Y. R., Morse, A. S., Anderson, B. D., and Belhumeur, P. N. (2004). Rigidity, computation, and randomization in network localization. In *INFOCOM*, volume 4, pages 2673–2684. IEEE.

Fang, X., Xie, L., and Li, X. (2023). Distributed localization in dynamic networks via complex laplacian. *Automatica*, 151:110915.

Fang, X., Xie, L., and Li, X. (2024). Integrated relative-measurement-based network localization and formation maneuver control. *IEEE Transactions on Automatic Control*, 69(3):1906–1913.

Filippov, A. F. (2013). *Differential equations with discontinuous righthand sides: control systems*, volume 18. Springer Science and Business Media.

Fischer, N., Kamalapurkar, R., and Dixon, W. E. (2013). Lasalle-yoshizawa corollaries for nonsmooth systems. *IEEE Transactions on Automatic Control*, 58(9):2333–2338.

Jing, G., Wan, C., and Dai, R. (2022). Angle-based sensor network localization. *IEEE Transactions on Automatic Control*, 67(2):840–855.

Khan, U. A., Kar, S., and Moura, J. M. (2009). Distributed sensor localization in random environments using minimal number of anchor nodes. *IEEE Transactions on Signal Processing*, 57(5):2000–2016.

Le-Phan, N.-M., Trinh, M. H., and Nguyen, P. D. (2023). Bearing-based network localization under randomized gossip protocol. In *12th International Conference on Control, Automation and Information Sciences*, pages 429–434. IEEE.

Le-Phan, N.-M., Trinh, M. H., and Nguyen, P. D. (2024). Randomized matrix weighted consensus. *IEEE Transactions on Network Science and Engineering*, 11(4):3536–3549.

Mehdifar, F., Bechlioulis, C. P., Hendrickx, J. M., and Dimarogonas, D. V. (2022). 2-d directed formation control based on bipolar coordinates. *IEEE Transactions on Automatic Control*, 68(7):4175–4190.

Shames, I., Bishop, A. N., and Anderson, B. D. (2012). Analysis of noisy bearing-only network localization. *IEEE Transactions on Automatic Control*, 58(1):247–252.

Su, H., Yang, Z., Zhu, S., Chen, C., and Yu, W. (2023). Bearing-based target entrapping control of multiple uncertain agents with arbitrary maneuvers. *IFAC-PapersOnLine*, 56(2):8821–8826.

Tang, Z., Cunha, R., Hamel, T., and Silvestre, C. (2020). Bearing leader-follower formation control under persistence of excitation. *IFAC-PapersOnLine*, 53(2):5671–5676.

Tang, Z., Cunha, R., Hamel, T., and Silvestre, C. (2021). Formation control of a leader–follower structure in three dimensional space using bearing measurements. *Automatica*, 128:109567.

Tang, Z. and Loría, A. (2022). Localization and tracking control of autonomous vehicles in time-varying bearing formation. *IEEE Control Systems Letters*, 7:1231–1236.

Teel, A. R. (1995). Semi-global stabilizability of linear null controllable systems with input nonlinearities. *IEEE Transactions on Automatic Control*, 40(1):96–100.

Trinh, M. H. and Ahn, H.-S. (2021). Finite-time bearing-based maneuver of acyclic leader-follower formations. *IEEE Control Systems Letters*, 6:1004–1009.

Trinh, M. H., Zhao, S., Sun, Z., Zelazo, D., Anderson, B. D., and Ahn, H.-S. (2018). Bearing-based formation control of a group of agents with leader-first follower structure. *IEEE Transactions on Automatic Control*, 64(2):598–613.

Van Tran, Q., Park, S.-H., and Ahn, H.-S. (2018a). Bearing-based formation control via distributed position estimation. In *IEEE Conference on Control Technology and Applications*, pages 658–663. IEEE.

Van Tran, Q., Trinh, M. H., Zelazo, D., Mukherjee, D., and Ahn, H.-S. (2018b). Finite-time bearing-only formation control via distributed global orientation estimation. *IEEE Transactions on Control of Network Systems*, 6(2):702–712.

Yang, Z., Chen, C., Zhu, S., Guan, X., and Feng, G. (2021). Distributed entrapping control of multiagent systems using bearing measurements. *IEEE Transactions on Automatic Control*, 66(12):657–664.

Yang, Z., Zhu, S., Chen, C., Feng, G., and Guan, X. (2020). Entrapping a target in an arbitrarily shaped orbit by a single robot using bearing measurements. *Automatica*, 113:108805.

Ye, M., Anderson, B. D., and Yu, C. (2017). Bearing-only measurement self-localization, velocity consensus and formation control. *IEEE Transactions on Aerospace and Electronic Systems*, 53(2):575–586.

Zhao, S., Li, Z., and Ding, Z. (2019). Bearing-only formation tracking control of multiagent systems. *IEEE Transactions on Automatic Control*, 64(11):4541–4554.

Zhao, S. and Zelazo, D. (2016). Localizability and distributed protocols for bearing-based network localization in arbitrary dimensions. *Automatica*, 69:334–341.

Zhao, S. and Zelazo, D. (2019). Bearing rigidity theory and its applications for control and estimation of network systems: Life beyond distance rigidity. *IEEE Control Systems Magazine*, 39(2):66–83.

Zhu, S., Lv, K., Yang, Z., Chen, C., and Guan, X. (2023). Bearing-based formation tracking control of nonholonomic mobile agents with a persistently exciting leader. *IEEE Transactions on Control of Network Systems*, 11(1):307–318.